Self-Propelled Intelligent Robotic Vehicle Based on Octahedral Dodekapod to Move in Active Branched Pipelines with Variable Cross-Sections

Sergey N. Sayapin, Anatoly P. Karpenko, Suan H. Dang

Abstract—Comparative analysis of robotic vehicles for pipe inspection is presented in this paper. The promising concept of self-propelled intelligent robotic vehicle (SPIRV) based on octahedral dodekapod for inspection and operation in active branched pipelines with variable cross-sections is reasoned. SPIRV is able to move in pipeline, regardless of its spatial orientation. SPIRV can also be used to move along the outside of the pipelines as well as in space between surfaces of annular tubes. Every one of faces of the octahedral dodekapod can clamp/unclamp a thing with a closed loop surface of various forms as well as put pressure on environmental surface of contact. These properties open new possibilities for its applications in SPIRV. We examine design principles of octahedral dodekapod as future intelligent building blocks for various robotic vehicles that can self-move and self-reconfigure.

Keywords—Modular robot, octahedral dodekapod, pipe inspection robot, spatial parallel structure.

I. INTRODUCTION

IT is well known that pipelines are pipes which are used for carrying oil, gas, and etc. over long distances. The pipeline can consist of underground, overhead, subsea pipeline sections, or a combination of these. The pipeline includes horizontal and vertical pipe sections with different branch pipes (pipe elbow, Y-fitting, T-branch, and etc.). The pipeline can contains some pipes with variable cross-section. The pipeline damage may lead to a leak of dangerous oil, gas, etc. A water leak can also be a problem. Therefore, pipeline inspection is an essential activity to better understand the condition of any pipeline, ultimately to ensure that all assets are fully operational with a long life cycle which can be well over 25 years since initial installation. It should be noted that some pipeline repairs and modification are inevitable and necessary during the course of an asset lifecycle. Robotic vehicles for pipe inspection and repair as necessary are needed where people cannot go, or where the hazards of human presence are great (smaller size, longer range, increased maneuverability, high level of irradiation, and etc.). Therefore, the main use of such robotic vehicles is nuclear power plants, conventional power plants, refineries, chemical and

petrochemical plant, offshore rigs, long distance city heating pipelines, food and drinks industries, communal waste water pipe systems, gas pipelines, etc. This type of the robotic vehicle is one of the fastest growing the fields of intelligent robotic vehicle of today. The types of inspection tasks are very different. As a result there are a large number of different robotic vehicles for pipe inspection which can be divided into three groups: inside [1]-[3], outside [4]-[7], and dual-purpose [8]-[13]. According to [1], existing pipe inspection robots can be classified by their different movement pattern into one or more of the seven main types, as shown in Fig. 1: pig type (a), wheel type (b), caterpillar type (c), wall press type (d), walking type (e), inchworm type (f), and screw type (g). These robots can also be categorized by their different locomotion methods: wheeled, inchworm, snake, and legged, as in [2].

Different types of robot motion in different pipeline bends are given in Fig. 2.
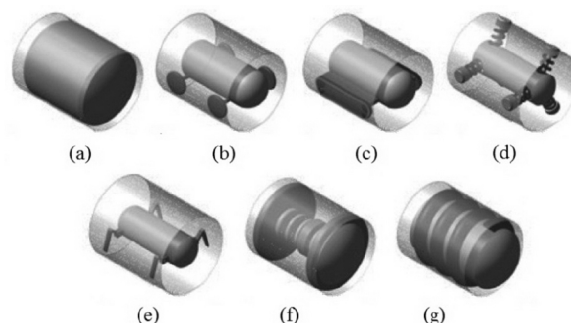

Fig. 1 Classification of in-pipe robots

Due to the complexity of the existing water pipeline distribution systems, it is essential for in-pipe robots to be able to handle such pipeline geometries (vertical pipes, pipe elbow, Y-fitting, T-branch, and etc.) [1]. Therefore making the passive approach (pig type) and number other approaches inadequate. From these approach only snake-robots and climbing parallel robots can be divided into dual-purpose (inside and outside). When considering design concepts for the proposed robot in this paper, snake locomotion method were dismissed due to their control complexity. Design of the climbing parallel robot (CPR) with six-degrees-of-freedom is given in Fig. 3 [4]. CPR can be used for inspection and manipulation works both on the outside of pipe (a) and inside of it, as shown in (b) and (c). The main features of this kind of robots are stiffness, high velocities, and high force-output-to

S. N. Sayapin is with the Institute for Machine Science named after A. A. Blagonravov of the Russian Academy of Science, 4 Maly Kharitonyevsky Pereulok, Moscow, 101990, Russia (Corresponding author, phone/fax: +7 (499) 135-61-46; e-mail: S.Sayapin@ rambler.ru).

A. P. Karpenko is with the Bauman Moscow State Technical University, 2-nd Baumanskaya, 5, Moscow, 105005, Russia (e-mail: apkarpenko@mail.ru).

S. H. Dang is with the Bauman Moscow State Technical University, 2-nd Baumanskaya, 5, Moscow, 105005, Russia (e-mail: rk6bmstu@mail.ru).

World Academy of Science, Engineering and Technology
International Journal of Mechanical and Mechatronics Engineering
Vol:9, No:12, 2015

manipulator-weight ratio, which make them suitable for climbing applications.

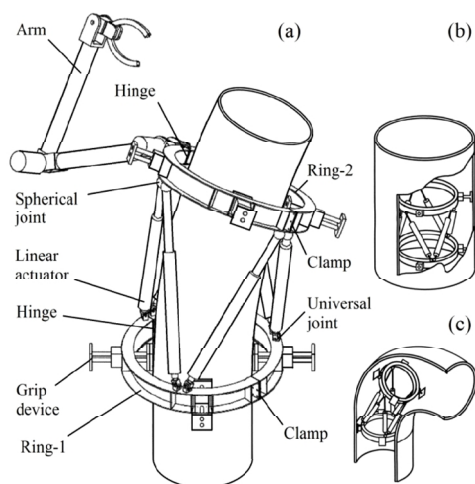Fig. 2 Different types of motion in elbow, T-, and Y-branches

Fig. 3 Design of the climbing parallel robot [4]

However, the side faces of CPR do not have the ability to clamp/unclamp a pipe or other thing with a closed loop surface of various forms as well as put pressure on environmental surface of contact. CPR cannot move on T- and Y-branches and along pipes with variable cross section. These and other limitations reduce the functional possibilities of CPR. The new concept of self-propelled intelligent robotic vehicle (SPIRV) for inspection and operation in active branched pipelines with variable cross-sections is presented below (Figs. 4 and 5).

II. DESCRIPTION OF SPIRV

SPIRV based on the octahedral dodekapod (from the Greek words dodeka meaning twelve and pod meaning foot or its counterpart leg) which is the parallel robotic mechanism with twelve degrees of freedom. Every one of its triangular faces is formed by linear drives that are connected with vertices of octahedron by spherical joints. As a result, all faces of the octahedral dodekapod can clamp/unclamp a thing with a closed loop surface of various forms as well as put pressure on environmental surface of contact. This feature opens new

functionality of the octahedral dodekapod versus a hexapod and others parallel spatial robots. The schematic view of the monomodule SPIRV (a) and the simplified structural scheme of the control system (b) are shown in Fig. 4. The structural scheme includes maximal number of sensors, radial stops and grippers. This number is dependent on the applications and it may be decreased. SPIRV is executed as the octahedral module 1. All ribs of the octahedron are executed as the rods with the linear drives 2 each of which have the axial force sensor 3, the medial force sensor 4, the relative displacement sensor 5, and the relative velocity sensor 6. The ends of the adjacent ribs are connected by the spherical joints in the points of octahedral module 7 of the octahedral module 1. The points of octahedral module 7 contain the radial stops and the middles of the rods contain the grippers (on Fig. 4 were not shown) each of which have the temperature sensor 8. The octahedral module 1 has 12 d.o.f., which is a spatial farm as soon as all linear drives 2 are turned off. All points of octahedral module 7 have the spatial position sensors 9 which are integrated with the three-axial acceleration sensors 10. The control system (CS) 11 includes: the neural computer 12, the software 13 and the digital-analog converter (DAC) 14. The inputs of CS 11 are connected to outputs of the analog-digital converter (ADC) 15 of sensors 3 and 4, ADC 16 of sensors 5, ADC 17 of sensors 9 and 10, ADC 18 of sensors 6, and ADC 19 of sensors 8. Outputs of CS 11 are connected to inputs of the software 13 and DAC 14. The outputs DAC 14 are connected to the power amplifier 20 which is connected to each of the linear drives 2.
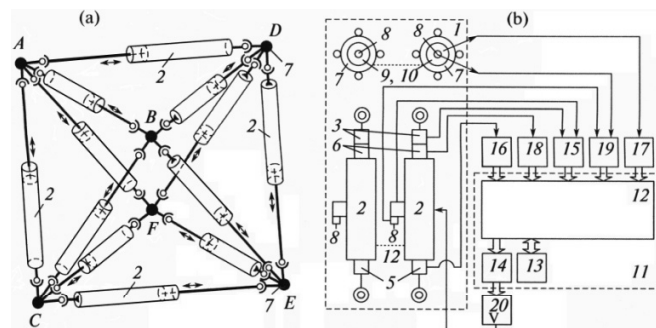

Fig. 4 Octahedral module of SPIRV (a) and its structure (b). [10]

The octahedral module 1 may be used as a base element not only at the monomodule SPIRV, but also at the multimodule ones. The radial stops and the grippers (on Fig. 4 were not shown) provide the transmission of the efforts from linear drives toward the internal and external contact surfaces. The force sensors 3, 4 and temperature sensors 8 provide the operative control of these efforts and temperature in the contact places. The spatial position sensors 9 with three-axial acceleration sensors 10 provide the operative control of the spatial position of points of octahedral module 7 and of vibration along each of axes of rods with linear drives 2. The relative displacement sensors 5 and the relative velocity sensors 6 of the linear drives 2 register their relative movements and velocities. Before using it we will have to

World Academy of Science, Engineering and Technology
International Journal of Mechanical and Mechatronics Engineering
Vol:9, No:12, 2015

place the octahedral module 1 in the inside or the outside of the closed surface and then carry out the necessary movements depending on requirement. The linear drives 2 and the CS 11 fulfill herewith the coordinated changes of the rib lengths of the octahedral module. As a result the points of octahedral module 7 have got spatial movement concerning a base system of coordinates. A geometrical invariability of the octahedral module 1 allows to define the spatial coordinates of all points of octahedral module 7 as a result of the measurement of the lengths of all rods and to control their spatial movements like as in Stewart's platform [11]. The sensors of the spatial position 9 allow herewith elevating a precision of these measurements. The neural computer 12 and the software 13 provide the control of real time.

SIRV movement in different kinds of pipes and along columns is shown in Fig. 5. The conditions and the algorithms for movements of SPIRV in straight pipes of constant and variable cross-sections with different bends are represented below (Figs. 5, 7 and 9).
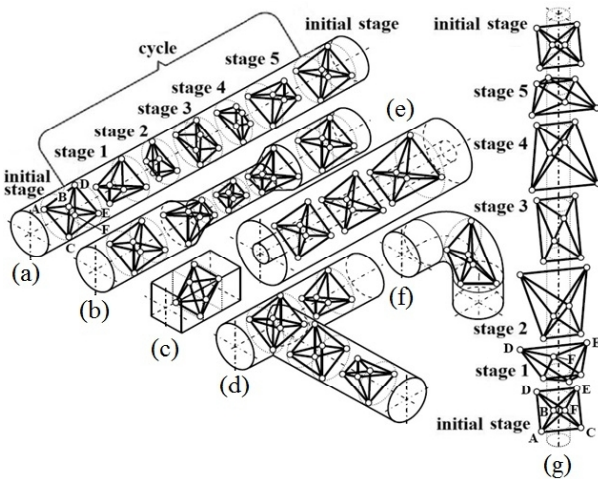

Fig. 5 SIRV movement in different kinds of pipes and along columns: terete or oval pipe (a), pipe with constant and variable cross-sections (b), quadrate pipe (c), T- or Y-branch (d), annular pipes (e), elbow (f), column (g)

III. THE ALGORITHMS FOR THE MOVEMENTS OF SPIRV IN THE PIPES OF CONSTANT AND VARIABLE CROSS-SECTIONS

A. Basic Parameters of Octahedral Dodekapod

The octahedral dodekapod, as shown in Fig. 6 (a) contains 6 spherical joints (vertices A, B, C, D, E, F) and 12 rods (ribs AB, BC, AC, DE, EF, DF, AD, AE, BD, BF, CE, CF) with linear drives.

The vertices A, B, C and D, E, F form two parallel triangular faces (ABC and DEF). The vertices A, B, C and D, E, F are the octahedral dodekapod's stops for a moving in the pipe. When one of the faces in the pipe is fixed, the other face moves by simultaneous changes in the lengths of rods AD, AE, BD, BF, CE, CF, as shown in Fig. 6 (b). It is assumed that during the motion of the octahedral dodekapod no slippage between stops and the pipe.

Basic notations, as shown in Figs. 6 (a) and (c):

- l_0, l_m - the minimum and maximum lengths of the rods of octahedral dodekapod;
- δ - the diameter of the spherical joints of octahedral dodekapod;
- l_S — the rod lengths of faces ABC and DEF at the time of contact their vertices with the inner surface of a pipe;
- H_{min} - the minimum distance between the faces ABC and DEF (the length of the side rods reaches the minimum length);
- H_{max} - maximum distance between the faces ABC and DEF (the length of the side rods reaches the maximum length);
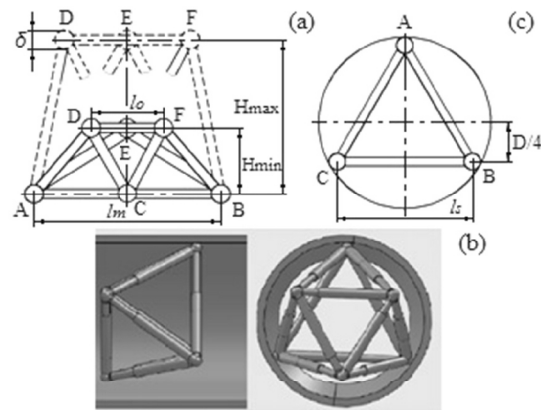- h_s - step of the movement of octahedral dodekapod, $l_0 < l_s < l_m$.

Fig. 6 Structure and basic notations of octahedral dodekapod in pipe constant cross-sections

B. The Algorithm for the Movement of Octahedral Dodekapod in Pipe of Constant Cross-Section

There is a cylindrical pipe with an internal diameter D and length L. Fixing dodekapod in the pipe during the movement is ensured by alternately fixing faces (ABC or DEF) through the elongate rods. A fixed face should be an equilateral triangle and perpendicular to the axis of symmetry of the pipe, as shown in Fig. 6 (c). A condition moving of the dodekapod in the pipe: the value l_s is in the range of possible lengths of the rods ($l_0 < l_s < l_m$); $l_s = 3^{0,5}D/2$, as shown in Fig. 6 (c). As a result we obtain the condition:

$$2l_0/\sqrt{3} \leq D \leq 2l_m/\sqrt{3} \qquad (1)$$

The algorithm for the movement of the octahedral dodekapod in pipe of constant cross-section, as shown in Fig. 7:

1) The initial lengths of rods and initial position of the spherical joints are assigned from conditions: $l_{AB}=l_{BC}=l_{CA}=l_{DE}=l_{EF}=l_{DF}=l_s=3^{0,5}D/2$; $l_{AF}=l_{BF}=l_{BD}=l_{CD}=l_{CE}=l_{AE}=l_m$.
2) The reduced length of rods AB, BC, CA from l_s to l_0.
3) The reduced length of rods AD, AE, BD. BF, CE, CF from l_m to l_0.
4) The increased length of rods AB, BC, CA from l_0 to l_s.
5) The reduced length of rods DE, EF, DF from l_s to l_0.

World Academy of Science, Engineering and Technology
International Journal of Mechanical and Mechatronics Engineering
Vol:9, No:12, 2015

6) The increased length of rods *AD, AE, BD. BF, CE, CF* from l_0. to l_m.

7) The increased length of rods *DE, EF, DF* from l_0 to l_s.

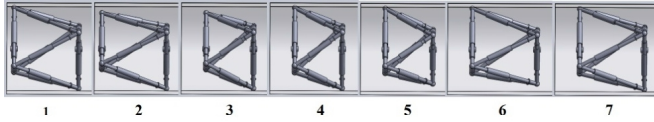8) A repeat of steps from second to seventh.

Fig. 7 The algorithm for the movement of octahedral dodekapod in pipe of constant cross-section

C. The Algorithm for the Movement of Octahedral Dodekapod in Pipe of Variable Cross-Section

Regarded pipe has three sections, as shown in Fig. 8. Two extreme sections have constant cross section (diameters D, d and lengths L_1, L_2), and the middle section has a variable cross-section (length Δ). The complexity of the problem is the possibility of collision of octahedral dodekapod with the inner wall of pipe in transition. It is therefore necessary to determine the ratio between the radii of the platform base and the steps of movement.
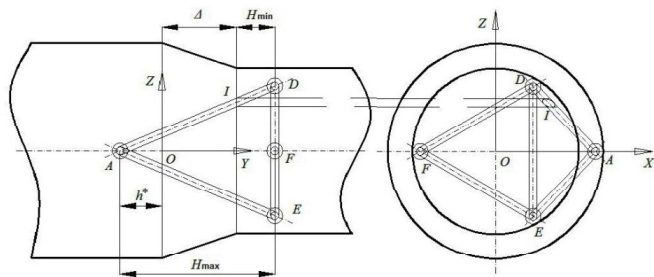

Fig. 8 The octahedral dodekapod in the middle section of pipe

The conditions for the movement in the transition: l_s is in the range of possible lengths of the rods ($2l_0/3^{0,5} \leq D$; $d \leq 2l_m/3^{0,5}$); $d_{I/OY} < d/2$.

Coordinates of spherical joints A, D:

$$A\left(\frac{D}{2} - \frac{\delta}{2}, -h^*, 0\right) \quad D\left(\frac{d-\delta}{2}, \Delta + H_m, \frac{\sqrt{3}}{4}d - \frac{\delta}{2}\right); \qquad (2)$$

$$\overrightarrow{A} = \left(\frac{d}{4} - \frac{D}{2}, \Delta + H_m + h^*, \frac{\sqrt{3}}{4}d - \frac{\delta}{2}\right);$$

$$\overrightarrow{A} = \frac{h^* + \Delta}{h^* + \Delta + H_m}\overrightarrow{A} = \left(\frac{h^* + \Delta}{h^* + \Delta + H_m}\left(\frac{d}{4} - \frac{D}{2}\right),\right.$$

$$\Delta + h^*, \frac{h^* + \Delta}{h^* + \Delta + H_m}\left(\frac{\sqrt{3}}{4}d - \frac{\delta}{2}\right);$$

$$\overrightarrow{O} = \overrightarrow{O} + \overrightarrow{A} = \frac{h^* + \Delta}{h^* + \Delta + H_m}\left(\frac{d}{4} - \frac{D}{2}\right) + \frac{D - \delta}{2},$$

$$\Delta, \frac{h^* + \Delta}{h^* + \Delta + H_m}\left(\frac{\sqrt{3}}{4}d - \frac{\delta}{2}\right);$$

$$d_{I/O} = \sqrt{(\frac{2\Delta - H_m}{\Delta}\left(\frac{d}{4} - \frac{D}{2}\right) + \frac{D-\delta}{2})^2 + (\frac{2\Delta - H_m}{\Delta}\left(\frac{\sqrt{3}}{4}d - \frac{\delta}{2}\right))^2} < \frac{d}{2}; (3)$$

If $h^* \geq 0$ ($H_{min} \leq \Delta$), then $h^* = \Delta - H_{min}$ and from (3):

$$d_{I/O} = \sqrt{(\frac{2\Delta - H_m}{\Delta}\left(\frac{d}{4} - \frac{D}{2}\right) + \frac{D-\delta}{2})^2 + (\frac{2\Delta - H_m}{\Delta}\left(\frac{\sqrt{3}}{4}d - \frac{\delta}{2}\right))^2} < \frac{d}{2}; (4)$$

If $h^* < 0$ ($H_{min} > \Delta$), then $h^* = H_{min} - \Delta$ and from (3):

$$d_{I/O} = \sqrt{(\frac{d + 2D - 4\delta}{8})^2 + (\frac{\sqrt{3}d - 2\delta}{8})^2} < \frac{d}{2}. \qquad (5)$$

The algorithm for the movement of the octahedral dodekapod in pipe of variable cross-section, as shown in Fig. 9:

1) The movement of the dodekapod near the middle section: the number of steps $N = L_1/h_s$, $h_s = H_{max} - H_{min}$; the length of rods of the faces *ABC* and *DEF* $l_{AB} = l_{DE} = 3^{0,5}(D-\delta)/2$; $l_{AF} = l_m$- the length of the side rods.
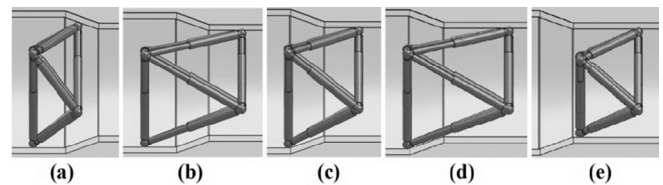

Fig. 9 The algorithm for the movement of the octahedral dodekapod in pipe of variable cross-section

2) The movement of the octahedral dodekapod forward with a step $h_{s1} = L_1 - Nh_s$; $l_{AB} = l_{DE} = 3^{0,5}(D-\delta)/2$. The face *DEF* of the dodekapod is installed in leading edge of middle section of pipe, as shown Fig. 9 (a).

3) If the conditions (2)-(5) are satisfied, then the octahedral dodekapod moves through the middle section of the pipe with step $h_{s2} = \Delta + H_{min}$; $l_{AB} = l_{DE} = 3^{0,5}(d-\delta)/2$, as shown Figs. 8 (b)-(d).

4) The octahedral dodekapod moves in through the extreme section of the pipe with step $h_s = H_{max} - H_{min}$; $l_{AB} = l_{DE} = 3^{0,5}(d-\delta)/2$, as shown Fig. 9 (e).

IV. Other Capabilities of SPIRV

The novel concept of SPIRV may be used also in many other fields. The examples of applications the Octahedral dodekapod and the new functional capabilities are established, e.g.:

1) Possibility of control over of physical-mechanical properties, geometrical shape of contact surface and displacement trajectory (Fig. 10).

2) Travel of long objects in pipe (Fig. 11).

3) Travel of object in pipe with possibility of vibroprotection and positioning (Fig. 12).

4) Possibility of hole drilling in the end of pipe wall (Fig. 13).

5) Possibility of battering in pipe of wall end (Fig. 14).

World Academy of Science, Engineering and Technology
International Journal of Mechanical and Mechatronics Engineering
Vol:9, No:12, 2015

6) Octahedral dodekapod can connect together, forming some novel mobile self-reconfigurable structures (swarm systems) for various applications [10].

Example of control of geometrical shape of contact surface by octahedral dodekapod is given in Fig. 10. In this mode, in the motion of the octahedral module *ABCDEF* (module 1, Fig. 4) of the adaptive mobile parallel spatial robot (Fig. 10), each longitudinal displacement of the rear face ΔABC and frontal face ΔDEF is preceded by alternating discrete rotations in both directions, with specified increment, relative to the direction of motion. For each discrete position, mechanical contact is established between the radial limiters at points 7 (Fig. 4) of those faces and the internal contact surface or between the radial limiters at the midpoints of the rods in the frontal and rear faces and the external constant surface. Their coordinates are determined in the basic coordinate system. These values permit judgments regarding the geometric form of the internal or external contact surfaces. The specified contact forces with the internal surface are determined from the readings of sensors 3; and the specified contact forces with the external surface are determined from the readings of sensors 4. The position of points 7 of the frontal and rear faces (ΔABC, ΔDEF) are determined from the readings of the relative displacement sensors 5 of linear drives 2 for the rods of the lateral faces and position sensors 9 at points 7.
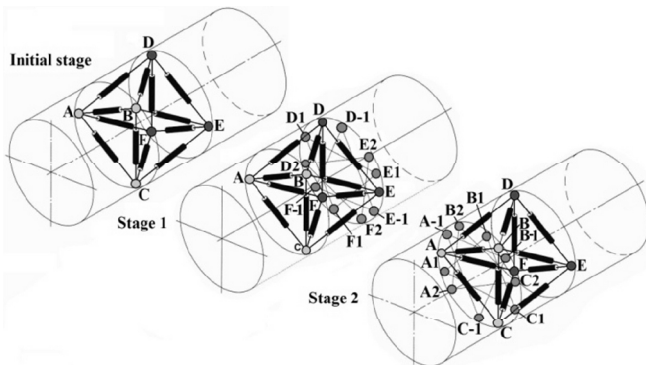

Fig. 10 Possibility of control over of physicomechanical properties, geometrical shape of contact surface and displacement trajectory

In mode of control of elastic properties of contact surface (Fig. 10), the radial limiters at points 7 (Fig. 4) of the faces come into contact with an internal surface, with a force specified by the readings from sensors 3. Then, their position is determined in the basic coordinate system on the basis of the readings from sensors 5 and 9. Next, the force on the radial limiters is increased to another specified value, and their position is determined in the basic coordinate system. This procedure is then repeated with the initial force. The difference between the coordinates of the radial limiters at points 7 permits judgments regarding the elastoplastic properties of the contact surface. At specified contact force between the radial limiters and the internal surface, the temperature is measured by means of sensors 8, and the electrical resistance between them is recorded. These readings permit judgments regarding the physical properties of the

contact surface. Analogously, the temperature and electrical resistance may be recorded for an external surface. Vibrational diagnostics may also be organized for an internal contact surface, with identification of the presence of mechanical defects (such as cracks in pipes). In that case, periodic acceleration of linear drives 2 for the rods of the rear or frontal faces permits impact and vibrational influence on the radial limiters at points 7 of these faces at the contact surface. Vibrational diagnostics of the object may then be based on the readings of acceleration sensors 10.

In Fig. 11, we show examples of the motion of round or oval objects by octahedral module *ABCDEF* without (a) and with (b) a guide system. In this mode, octahedral module 1 (Fig. 4) moves within a closed surface and fixes the frontal face (ΔDEF, say). The end of the extended object (such as pipe, rod, or cable) is placed in the rear face ΔABC (Fig. 11, initial position), and linear drives 2 are turned on in reverse.
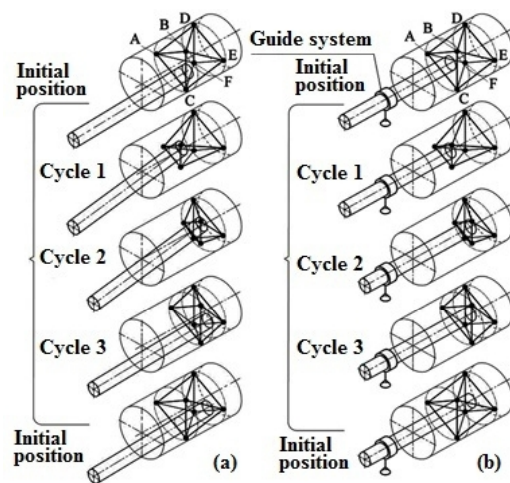

Fig. 11 Motion of extended rounded objects within a closed surface by the octahedral module *ABCDEF*

The length of the rods in the rear face is reduced until the object is captured by force specified by the readings of the force sensors 4 at the radial limiters at the midpoints of the rods in rear face ΔABC. Then, at a command from control system 11, linear drives 2 are switched off, and the coordinates of points 7 are determined, in the basic coordinate system. After the object is fixed (Fig. 11, cycle 1), coordinated decrease in length of the rods in the lateral faces (ΔABD, ΔBDE, ΔBCE, ΔCEF, ΔACF, ΔADF) shifts the rear face ΔABC together with the object into the closed surface by some fixed distance, which is recorded with respect to the basic coordinate system (Fig. 11, cycle 2). Then the length of the rods in the rear face is increased until the radial limiters at the midpoints, together with the object, are completely released (Fig. 11, cycle 3) and the object is unable to move in the opposite direction (Fig. 11 (a), cycle 3). Then the length of the rods in the lateral faces is increased to its initial value (Fig. 11, initial position). Thereafter, the motion of the object is repeated as many times as is necessary, and the total length traversed at the end of the process is determined. Note that the

World Academy of Science, Engineering and Technology
International Journal of Mechanical and Mechatronics Engineering
Vol:9, No:12, 2015

motion of the object may be conducted without (Fig. 11 (a)) or with a guide system, as shown in Fig. 9 (b). Without a guide system, additional effort is required to prevent inverse motion of the object in cycle 3. With a guide system (Fig. 11 (b)), that is unnecessary. If required, motion in a combination of modes 1 and 4 is possible. In that case, the object will move with simultaneous independent motion of octahedral module 1 within the closed system. In contrast to mode 4 (Fig. 11 (b)), the length of the rods in the rear face $\triangle ABC$ increases not until the object is released but until fixing of points 7 of the rear face $\triangle ABC$ at the closed internal surface with specified force, in accordance with the readings of sensors 3. Then linear drives 2 are switched off, and the coordinates of points 7 are calculated from the readings of sensors 5 and 9. Next, at a command from control system 11, linear drives 2 of rods in the frontal face $\triangle DEF$ are switched on in reverse, and their length is reduced until capture of the object by the radial limiters at the midpoints of these rods, with a force specified by the readings from sensors 4. Then linear drives 2 are switched off, and the coordinates of points 7 are calculated from the readings of sensors 5 and 9. At that point, the length of the rods in the lateral faces is increased, and the object is moved within the closed surface. Then the length of the rods in the frontal face $\triangle DEF$ is increased until the points 7 of the rear face $\triangle ABC$ are fixed at the reduced length of the closed internal surface with specified force, in accordance with the readings of sensors 3. Then linear drives 2 are switched off, and the coordinates of points 7 are calculated from the readings of sensors 5 and 9. Thus, in this mode, not only the extended object but the octahedral module 1 will be moved. As a result, the distance traveled by the object relative to the closed internal surface will be increased, with a fixed number of cycles (operations).

Motion of objects in the pipe by means of paired octahedral modules, with simultaneous positioning and vibrational protection of the objects (Fig. 12). In this mode, the octahedral modules are paired to form of a common face $\triangle ABC$. One octahedral module ($ABCDEF$) performs motion over a closed internal surface of the pipe, analogously to movement of octahedral dodekapod in pipe of constant cross-section (Fig. 7). The other octahedral module captures the object, analogously to the capture of the long objects in pipe (Fig. 11). The second module also positions the object and ensures vibrational protection during motion over the closed internal surface. The capture force and spatial position of the object, as well as the impact and vibrational influence of octahedral module $ABCDEF$ on the octahedral module with the object are monitored by means of force sensors 4 (Fig. 4), spatial position sensors 9 (Fig. 4), and three-axial acceleration sensors 10 (Fig. 4) mounted on radial supports of the rear face (the common face of the moving octahedral module and the clamping octahedral module) of the clamping module, as well as the relative displacement sensors 5 (Fig. 4) and relative velocity sensors 6 (Fig. 4) mounted at the rods of the lateral faces. Vibrational protection of the object relies on the linear drives 2 (Fig. 4) in the rods of the lateral faces of the clamping module. It involves coordinated change in the length of those

rods at a command from control system 11 (Fig. 4), on the basis of the readings of sensors 10 (Fig. 4) mounted at points 7 (Fig. 4) of the frontal and rear faces of the clamping module and also sensors 5 (Fig. 4) and 6 (Fig. 4) at each of the rods of the lateral faces of the clamping module.
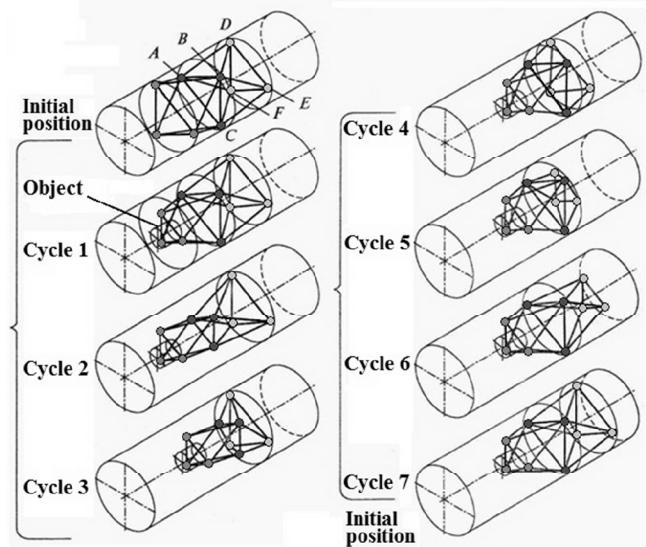

Fig. 12 Motion of object in pipe with possibility of vibroprotection and positioning by double octahedral dodekapod

Rotation and supply of a machining tool (a drill or bit, for instance) by means of octahedral module $ABCDEF$ (Fig. 13). In this case, the tailpiece of the tool takes the form of a crankshaft with a rotating bush at the end that is incapable of axial motion. (The rotating bush is not shown in Fig. 13.) The rotating bush is clamped by the radial limiters at points of the rods in the frontal face. Each limiter may be rigidly connected with one section of a three section bush intended for capture of the rotating tailpiece bush. The required force is determined on the basis of the sensors 4 in the frontal face. The radial limiters at the rear face are fixed at the internal contact surface, as in previous modes. Then, coordinated change in the length of the rods at the lateral faces brings the cutting section of the tool to the machining point, fixes the axis of tool rotation, and ensures the required cutting force, determined from the readings of sensors 3 at the rods of the lateral faces.

Next, coordinated change in the length of the rods at the lateral faces moves the axis of rotation of the clamped bush over a circle perpendicular to the axis of rotation; the circle radius is equal to the crankshaft radius. In tool rotation, coordinated increase in length of the rods at the lateral faces ensures its longitudinal supply with specified force; the generation of impact and vibration effects is possible in combination with tool rotation. In that case, the spatial position, cutting force, and impact and vibration effects are monitored by means of sensors 9 and 10 (Fig. 4) at the radial limiters of the frontal face and sensors 3, 5, and 6 (Fig. 4) at the rods in the lateral faces. The axis of tool rotation may be coaxial with the symmetry axis of octahedral module 1 (Fig. 13 (a) or eccentric (Fig. 13 (b)).
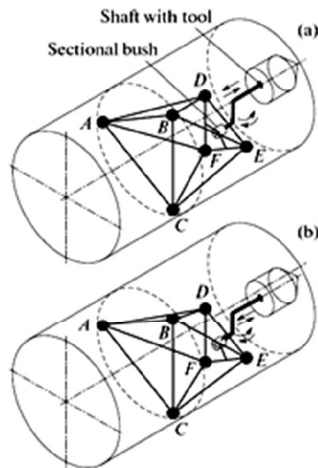
World Academy of Science, Engineering and Technology
International Journal of Mechanical and Mechatronics Engineering
Vol:9, No:12, 2015

Fig. 13 Rotation of a machining tool by means of octahedral module *ABCDEF*: (a) rotation coaxial with the module's symmetry axis; (b) eccentric rotation

Organization of impact and vibration effects by a slotting tool on the end surface (Fig. 14) of a tubular profile by means of octahedral module 1 (Fig. 4).
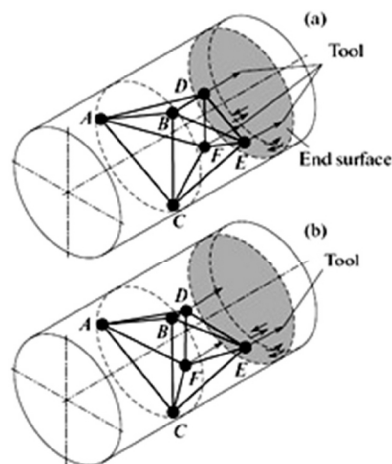

Fig. 14 Organization of simultaneous impact and vibrational effects on the end wall by slotting tools (a) and one time impact (b)

In this mode, the slotting tools are established at each point of the frontal face. (The clamping of the slotting tool's tailpiece is not shown in Fig. 14.) The radial limiters of the rear face are fixed at the internal contact surface as in previous modes. Then, coordinated change in the length of the rods at the lateral faces brings the working sections of the slotting tools into contact with the end surface at the machining site, and machining begins at specified frequency, amplitude, and force. In one time or double action, where necessary, the sequence of action may be modified. In each case, the spatial position, cutting force, and magnitude of the tools' impact and vibration effects are monitored by means of sensors 9 and 10 (Fig. 4) at the radial limiters of the frontal face and by sensors 3, 5, and 6 (Fig. 4) at the rods of the lateral faces. Real time operation is possible thanks to the use of a control system 11 based on neural computer 12 and corresponding software 13 (Fig. 4).

The proposed adaptive mobile parallel spatial robot may be used at the macroscopic level for use on land, underground, underwater, in medicine, and in the aerospace industry. It may also be used at the microscopic level. This research provides the basis for the development of up to date parallel spatial robots and for the expansion of their functional capabilities.

REFERENCES

[1] S. G. Roh and H. R. Choi, "Development of Differntail-Drive In-pipe Robot for Moving Inside Urban Gas Pipelines," *IEEE Trans. on Robotics*, vol. 21, no. 1, pp. 1-17, February 2005.

[2] V. G. Gradetsky, M. M. Knyazkov, L.F. Fomin, and V. G. Chashchukhin, *Miniature robot mechanics.* Moscow: Nauka, 2010.

[3] A. Bekhit., A. Dehghani, R. Richardson, "Kinematic Analysis and Locomotion Strategy of a Pipe Inspection Robot Concept for Operation in Active Pipelines," *International Journal of Mechanical Engineering and Mechatronics*, vol. 1, issue 1, pp. 15-27, 2012.

[4] M. Almonacid, R. J. Saltarén, R. Aracil, and O. Reinoso, "Motion Planning of a Climbing Parallel Robot," *IEEE Trans. on Robotics and Automation*, vol. 19, no. 3, pp. 485-489, June 2003.

[5] R. Saltaren, R. Aracil, and O. Reinoso, "Analysis of Climbing Parallel Robot for Construction Applications," *Computer-Aided Civil and Infrastructure Engineering*, vol. 19, pp. 436-445, 2004.

[6] S. Sakamoto, F. Hara, H. Hosokai, et. al. "Parallel-Link Robot for Pipe," *Industrial Electronics Society, 2005. IECON 2005. 31st Annual Conference of IEEE*, 6-10 Nov. 2005, pp. 345-350.

[7] M. Urdaneta, C. Garcia, G. Poletti, et. al. "Development of a Novel Autonomous Robot for Navigation and Inspect in Oil Wells," *Control Engineering and Applied Informatics. J.*, vol. 14, no. 3, pp. 9-14, 2012.

[8] R. Saltaren, R. Aracil, O. Reinoso and E. Yime, "Climbing with Parallel Robots," in *Bioinspiration and Robotics: Walking and Climbing Robots*, Maki K. Habib, Ed., Vienna, Austria, EU: I-Tech, 2007, pp. 209-226.

[9] S. N. Sayapin and A.V. Sineov, "Adaptive mobile 3D manipulator robot and method of organizing displacements and control over physical-mechanical properties, geometrical shape of contact surface and displacement trajectory hereby," Russian Federation Patent 2 424 893, January 11, 2009 (in Russian).

[10] S. N. Sayapin, "Parallel spatial robots of dodecapod type," *Journal of Machinery Manufacture and Reliability*, Allerton Press, USA, vol. 41, no. 6, pp. 457-466. Dec. 2012.

[11] S. Sayapin, A. Karpenko, and D. X. Hiep, "Dodekapod as universal intelligent structure for adaptive parallel spatial self-moving modular robots," in *Nature-Inspired Mobile Robotics. Proceedings of the 16th International Conference on Climbing and Walking Robots and the Support Technologies for Mobile Machines*, Editors: Kenneth J. Waldron, Mohammad O. Tokhi, Gurvinder S. Virk, Singapore: World Scientific, 2013, pp. 163-170.

[12] F. Enner, D. Rollinson, and H. Choset, "Motion Estimation of Snake Robots in Straight Pipes," in *Proc. IEEE International Conference on Robotics and Automation (ICRA)*, Karlsruhe, Germany, May 6-10, 2013, pp. 5148-5153.

[13] S. N. Sayapin, A. P. Karpenko, and S. H. Dang, "Universal adaptive spatial parallel robots of module type based on the Platonic solids," in *Proc. Annu. World Congress on Engineering*, London, 2014, pp. 1365-1370.